

Title Page

***CYP2C9*1B* promoter polymorphisms, in linkage with *CYP2C19*2*, affect
phenytoin auto-induction of clearance and maintenance dose**

Amarjit S Chaudhry, Thomas J Urban, Jatinder K Lamba, Angela K Birnbaum, Rory P Remmel,
Murali Subramanian, Stephen Strom, Joyce H You, Dalia Kasperaviciute, Claudia B Catarino,
Rodney A Radtke, Sanjay M Sisodiya,
David B Goldstein and Erin G Schuetz

Department of Pharmaceutical Sciences, St. Jude Children's Research Hospital, Memphis, TN,
U.S.A. (A.S.C., J.K.L., and E.G.S); Center for Human Genome Variation, Institute for Genome
Sciences and Policy, Duke University, Durham, NC, U.S.A. (D.B.G. and T.J.U.);
Departments of Experimental and Clinical Pharmacology and Medicinal Chemistry, University
of Minnesota, Minneapolis, MN, U.S.A. (J.K.L., A.K.B., R.P.R., and M.S.); Department of
Pharmaceutical Sciences, School of Pharmacy, University of Pittsburgh, Pittsburgh, PA, U.S.A.
(S.S.); School of Pharmacy, Faculty of Medicine, The Chinese University of Hong Kong, Hong
Kong, China (J.H.Y.); Department of Clinical and Experimental Epilepsy, UCL Institute of
Neurology, Queen Square, London, WC1N 3BG UK, (R.S., D.K., C.B.C., S.M.S.); and
Department of Medicine (Neurology), Duke University Medical School, Durham, NC, U.S.A.
(R.R.)

Running Title Page

- a) Running Title: *CYP2C9* polymorphisms affect phenytoin clearance and dosing
- b) Corresponding Author: Erin G. Schuetz, Ph.D., Department of Pharmaceutical Sciences, St. Jude Children's Research Hospital, 262 Danny Thomas Place, Memphis, TN 38105; PH: (901) 595-2205; Fax: (901) 595-3125; Email: erin.schuetz@stjude.org
- c) Number of Text Pages: 24
Number of Tables: 2
Number of Figures: 7
Number of References: 36
Number of words in Abstract: 200
Number of words in Introduction: 728
Number of words in Discussion: 1,729
- d) List of non-standard Abbreviations: PXR, pregnane X receptor; CAR, constitutive androstane receptor; YY1, Ying Yang 1 transcription factor; LD, linkage disequilibrium; PHT, phenytoin = 5,5-Diphenylhydantoin, 5,5-Diphenylimidazoline-2,4-dione; p-HPPH, 5-(4'-hydroxyphenyl)-5-phenylhydantoin; AED, antiepileptic drug; VAR, variant; WT, wild type; HAP, haplotype; -2663delTG, designation used by Veenstra et al. (2005) but equivalent to the -2665_-2664delTG designation used by some others; *CYP2C9*1B*, designation used by Veenstra et al. (2005) but identical to the *CYP2C9*1D* haplotype described by Kramer et al. (2008).
- e) recommended section assignment: Metabolism, Transport and Pharmacogenomics

Abstract

The commonly prescribed antiepileptic drug phenytoin has a narrow therapeutic range and wide inter-individual variability in clearance explained partially by CYP2C9 and CYP2C19 coding variants. After finding a paradoxically low urinary phenytoin metabolite (S)/(R) ratio in subjects on phenytoin maintenance therapy with a *CYP2C9**1/*1 & *CYP2C19**1/*2 genotype, we hypothesized that CYP2C9 regulatory polymorphisms (rPMs), G-3089A and -2663delTG, in linkage disequilibrium with *CYP2C19**2 were responsible. These rPMs explained as much as 10% of the variation in phenytoin maintenance dose in epileptic patients, but were not correlated with other patients' warfarin dose requirements or with phenytoin metabolite ratio in human liver microsomes. We hypothesized the rPMs affected CYP2C9 induction by phenytoin, a PXR and CAR activator. Transfection studies showed CYP2C9 reporters with wild-type versus variant alleles had similar basal activity but significantly greater PHT induction by co-transfected PXR, CAR and Nrf2 and less YY1 repression. Phenytoin induction of CYP2C9 was greater in human hepatocytes with the CYP2C9 wild-type vs. variant haplotype. Therefore, CYP2C9 rPMs affect phenytoin-dependent induction of CYP2C9 and phenytoin metabolism in humans, with an effect size comparable to that for *CYP2C9**2 and *2C9**3. These findings may also be relevant to the clinical use of other PXR, CAR and Nrf2 activators.

Introduction

Phenytoin (PHT, 5,5-diphenylhydantoin) is among the most frequently prescribed antiepileptic drugs (AEDs). Among the older AEDs, the prevalence of use in the United States is: PHT>valproic acid>carbamazepine>phenobarbital (52%, 19%, 11% and 7%, respectively). The use of phenytoin is highest among the elderly population, those most likely to be taking other medications metabolized by CYP2C9. For example, it is estimated that 10.5% of nursing home residents had one or more AED orders, a prevalence 10 times greater than that found in the community (Garrard et al., 2007; Leppik, 2007). Although newer AEDs that may have fewer side effects have come on the market, PHT continues to occupy an important role in the pharmacological treatment of epilepsy, particularly for patients on long standing PHT-containing regimens that may have required months to years of modification of drug regimens and doses to achieve optimal control of their disease.

Phenytoin demonstrates a large inter-individual variation in metabolism and has a narrow therapeutic index, and hence is difficult to administer effectively. Previous studies have consistently demonstrated reduced *in vivo* PHT metabolism and reduced clinical dose requirements for PHT in patients carrying protein sequence-altering genetic variants of the enzymes *CYP2C9* and *CYP2C19*. These enzymes metabolize PHT to a mixture of (*R*) and (*S*) stereoisomers of the inactive metabolite 5-(4'-hydroxyphenyl)-5-phenylhydantoin (*p*-HPPH). The most commonly occurring *CYP2C9* variant alleles are *CYP2C9**2, a C430T leading to Arg144Cys, and *CYP2C9**3 A1075T leading to Ile359Leu (Bhasker et al., 1997; Stubbins et al., 1996; Sullivan-Klose et al., 1996). An *in vitro* kinetic study in insect cells showed that recombinant *CYP2C9**2 and *CYP2C9**3 exhibited a 1.5-fold and 20-fold decrease in catalytic efficiency, respectively, relative to *CYP2C9**1, in formation of (*S*)-pHPPH (Rettie et al., 1999). The *CYP2C19**2 variant allele, a G681A transition in exon 5, creates a cryptic splice

site and forms a truncated defective protein. It is the major genetic defect accounting for 75 to 85% of CYP2C19 poor metabolizers (de Morais et al., 1994).

Because of its narrow therapeutic range, genotyping of CYP2C19 in addition to CYP2C9 could theoretically be used to optimize the dosage of phenytoin. The *CYP2C9*2*, *CYP2C9*3* and *CYP2C19*2* alleles have all been shown to affect PHT plasma concentration and toxicity (Desta et al., 2002; Aynacioglu et al., 1999; Tate et al., 2005). For example, the mean 12 h concentration of PHT in serum after a 300 mg dose to healthy Turkish volunteers was significantly higher (26-37%) in patients with even one *CYP2C9*2* or *CYP2C9*3* allele compared to WT subjects (Aynacioglu et al., 1999). In European epileptic patients on PHT, the *CYP2C9*3* allele showed a significant association with maximum PHT dose (Tate et al., 2005).

Although PHT is metabolized to p-HPPH by both CYP2C9 (90%) and CYP2C19, CYP2C9 demonstrates high prochiral stereoselectivity yielding an *S/R* ratio of 43-44. In contrast, CYP2C19 has low prochiral selectivity, yielding a *S/R* ratio of 1.2-1.3 (Fig 1A) (Kupfer and Preisig, 1984; Browne and Leduc, 2002; Bajpai et al., 1996). Although it was hypothesized (Ieiri et al., 1997; Argikar et al., 2006) that the (*S*)/(*R*) p-HPPH ratio could be used as a phenotypic measure of CYP2C9 activity, the results from two in vivo studies testing this idea have been paradoxical. For example, twelve and twenty-four hour urine samples from 45 epilepsy patients taking PHT under steady-state conditions analyzed for mean urinary p-HPPH (*S*)/(*R*) ratios in subjects homozygous for *CYP2C19*1/*1* was 24.2 ± 3.1 . Heterozygotes for the defective *CYP2C9*2* and *CYP2C9*3* alleles demonstrated lower values of 11.1 ± 3.3 and 2.7 ± 0.6 , respectively. However, unexpectedly, normal homozygotes for *CYP2C9*1/*1* but heterozygous for *CYP2C19*2* had a mean (*S*)/(*R*) ratio as low as 12.9 ± 1.7 instead of the expected range of 30-40 (Argikar et al., 2006). A high (*S*)/(*R*) ratio was expected in these subjects because CYP2C9-mediated metabolism would be expected to

predominate in *CYP2C19**2 poor metabolizers. We hypothesized that some undetected *CYP2C9* variation, in LD with *CYP2C19**2, was affecting PHT elimination.

Here we describe two genetic variants in the extended promoter of *CYP2C9*, -3089G>A and -2663delTG, in strong linkage disequilibrium with *CYP2C19**2, and demonstrate that these variants explain the paradoxically low (S)/(R) ratio in *CYP2C19**2 carriers. We show that these polymorphisms are strongly associated with phenytoin dose requirements in patients with epilepsy on PHT maintenance therapy, and that these variants are causal for reduced PHT metabolism through their effects on PHT-sensitive autoinduction of *CYP2C9*. These findings may have direct relevance to the clinical use of PHT and potentially other *CYP2C9* inducers.

Methods

Materials. QuikChange II XL site-directed mutagenesis kit was obtained from Stratagene (La Jolla, CA). TRIzol and Superscript reverse transcription-polymerase chain reaction (PCR) system were from Invitrogen (Carlsbad, CA). The luciferase assay system, β -galactosidase assay system, TNT quick coupled transcription/translation system, and PCR master mix were purchased from Promega (Madison, WI). High-purity plasmid purification kits and DNeasy tissue kit were supplied by QIAGEN (Valencia, CA). Trypsin, penicillin, streptomycin, cell culture minimal essential media were purchased from Gibco (Carlsbad, CA). Fetal bovine serum was purchased from HyClone (Logan, UT). DMSO and PHT were purchased from Sigma-Aldrich (St. Louis, MO). The transfection reagent Turbofectin 8, YY1 expression and Nrf2 expression plasmids were procured from Origene (Rockville, MD). γ - 32 P-ATP and 35 S-methionine were supplied by PerkinElmer (Waltham, MA). Exonuclease 1 and shrimp alkaline phosphatase were from USB Corp. (Cleveland, OH). FirstChoice[®] RLM-RACE Kit was purchased from Ambion/Applied Biosystems (Chicago, IL). Custom oligonucleotide synthesis and DNA sequencing was done by the Hartwell Center for Bioinformatics & Biotechnology at St. Jude Children's Research Hospital, Memphis, TN.

In silico analysis of the *CYP2C9* and *CYP2C19* genes. Databases screened for potential candidate SNPs in *CYP2C9* which are in LD with *CYP2C19**2: HapMap, <http://www.hapmap.org/> and Perlegen, <http://genome.perlegen.com/>. Web-based bioinformatic tools Nubiscan (<http://www.nubiscan.unibas.ch>) and Transfac (<http://hcfac.transfac/cgi-bin/biobase/transfac/11.4/bin/start.cgi>) were used to identify whether polymorphisms altered transcription factor binding sites.

Procurement of liver tissue. Human liver studies were approved by the St Jude Children's Research Hospital and University of Pittsburgh Institutional Review Boards. Human liver tissue (n=28) was processed through the St Jude Liver Resource at St. Jude Children's Research Hospital and was provided by the Liver Tissue Procurement and Distribution System (NIH Contract #N01-DK-9-2310) and by the Cooperative Human Tissue Network. RNA from donor livers was used to analyze the expression of CYP2C9 as well as to prepare cDNA to study the polymorphic splicing events by amplifying full length cDNA. DNA from donor livers was used to genotype for *CYP2C9**2, *CYP2C9**3, *CYP2C9* -3089G>A, *CYP2C9*-2663delTG and *CYP2C19**2.

mRNA quantification. Total RNA was isolated from liver or human hepatocytes with TRIzol. First-strand cDNA was prepared using oligo (dT) primers [Invitrogen, Superscript reverse transcription-polymerase chain reaction (PCR) system]. Real-time PCR quantitation of *CYP2C18* like Ex1/ 2C9 Ex2 chimera, *CYP2C9*, *CYP2C19*, *CYP3A4* mRNA and the housekeeping control glyceraldehyde-3- phosphate dehydrogenase was carried out using the QuantiTect SYBR Green PCR kit (Qiagen, Valencia, CA) according to the manufacturer's instructions. cDNA was analyzed in duplicate by quantitative real-time PCR on an ABI PRISM 7900HT Sequence Detection System (PE Applied Biosystems, Foster City, CA). Primers used for real-time quantification are provided in Supplemental Table 1. Specificity of amplification was confirmed in each case by performing melt curve analysis and agarose gel electrophoresis. The averaged Ct values were analyzed by the comparative Ct method to obtain relative mRNA expression levels.

Genotyping of *CYP2C9* and *CYP2C19* alleles. DNA from human livers was isolated using a DNeasy tissue kit. PCR was performed using 50 ng of genomic DNA template and 1 μ M of

each primer in a 25 μ L reaction volume using PCR master mix from Promega. Genotyping for *CYP2C9**2, *CYP2C9**3, *CYP2C9* -3089G>A, *CYP2C9*-2663delTG and *CYP2C19**2 was performed by direct DNA sequencing of the specific PCR amplified fragments. The primers were used for PCR amplification and DNA sequencing and are listed in Supplemental Table 1.

Epilepsy Study Population. The patient population included adult individuals of primarily European ancestry enrolled in a retrospective observational study of adult and pediatric chronic epilepsy patients followed by epileptologists at Duke University Medical Center (DUMC) (n=79), and the National Hospital for Neurology and Neurosurgery, University College London Hospital (UCLH) (n = 94). Studies were performed under protocols approved by the appropriate local Institutional Review Boards. Informed consent was either obtained from each patient or from the patients' parent or caregiver when it was not possible to obtain consent from the patient directly. A DNA sample was obtained from each patient, and medical records were reviewed retrospectively. Selected clinical data including a comprehensive past medical history and demographic information, epilepsy diagnosis, seizure type and frequency, drug initiation and stop dates, and adverse effects from AEDs were recorded in a relational database (InForm). We tested whether concomitant anti-epileptic medications, or any individual AED in particular, was associated with PHT maintenance dose, however, these variables did not significantly predict PHT dose requirements. Thus, we treated all individuals achieving the maintenance dose definition as a group, and ignored the potential influence of concomitant medications as a practical measure in our analysis. Genotyping for *CYP2C9**2, *CYP2C9**3 and *CYP2C9* -3089G>A was performed using Taqman MGB genotyping assays (Applied Biosystems, Inc., Foster City, CA, USA).

Phenotyping/Phenotype Definitions. Maintenance dose was defined as any prescribed dose that remained unchanged for two consecutive clinic visits, not including the initial (referral) visit. If this definition was met more than once for the same drug and patient, the dose that was maintained for the longest period of time was selected as the maintenance dose. It was anticipated that the maintenance dose would tend to reflect, in a quantitative manner, the liability toward seizure control by a given drug for a particular patient, whereas the maximum dose will tend to be limited by the tolerability of the drug, although both maintenance dose and maximum are likely to be influenced by both efficacy and tolerability.

Chinese patients on warfarin. This study received human subject approval from the Chinese University of Hong Kong-New Territories East Cluster Clinical Research Ethics Committee. After informed consent was obtained, a cohort of Chinese patients who had warfarin therapy initiated for indications of moderate intensity anticoagulation (target INR=2-3) were recruited at the anticoagulation clinic of the Prince of Wales Hospital in Hong Kong. Exclusion criteria included concurrent use of drugs known to interfere with warfarin metabolism, impaired hepatic function (>1.5 times upper normal limit of serum aminotransferases) or renal function (serum creatinine >120 $\mu\text{mol/L}$), and patients who had received warfarin for less than three months. A 5 mL blood sample was drawn for genotyping during a regularly scheduled clinic visit. Complete warfarin dosing information was retrieved from medical records to determine stable warfarin dose, defined as three INR measurements within target range, at the same mean daily dose, following consecutive clinic visits.

Human liver microsomes. Human liver microsomes were prepared from *CYP2C19**2 and *CYP2C9* -3089G>A genotyped samples (n=14) and analyzed for the formation of (S) and (R) p-HPPH. Microsomal incubations consisted of 100 μ L protein (1.25 mg protein/mL), 100 μ L 25 mM MgCl₂, 100 μ L 250 mM TRIS buffer (pH 7.4 at 37 °C), and 100 μ L 50 μ M PHT (10 μ M final concentration). The above mixture was preincubated at 37 °C for 2 min in a shaking water bath set at 30 rpm, and 100 μ L 5 mM NADPH were added to initiate the reaction. The reaction was stopped after 45 min by adding 100 μ L 20% TCA. Production of p-HPPH under these conditions was linear with respect to time and protein concentration. The samples were next placed on ice for 30 min to complete precipitation of the protein, followed by centrifugation at 13,000 x g for 10 min. An aliquot of the supernatant (500 μ L) was then subjected to solid phase extraction on Phenomenex Strata-X (30 mg) columns. Low speed (50 x g) centrifugation for 30 sec was used to elute the solutions and samples through the cartridge in a Forma Scientific (Model # 5681) swinging bucket centrifuge. The columns were activated with 1 mL methanol, followed by conditioning with 1 mL 10 mM ammonium formate buffer (pH 3). The sample was next added to the column and allowed to stand for 2 min prior to centrifugation. The cartridges were then washed with 1 mL 2% methanol in buffer, followed by two washes of 1 mL buffer solution. The cartridges were allowed to stand for 3 min before centrifugation. Sample elution was carried out with two 1 mL washes of acetonitrile. The final centrifugation was carried out at 75 x g for 1 min. All eluants were collected and dried under nitrogen at 40 °C, followed by reconstitution in 100 μ L 50% acetonitrile and 50% ammonium acetate buffer (10 mM). The reconstituted samples were centrifuged at 10,000 x g for 10 min in a Beckman microcentrifuge, and 30 μ L sample was injected into the LC-MS for analysis. Separation of R- and S-p-HPPH was accomplished with a Nucleodex beta-OH chiral column (200 mm x 4.6 mm) (Macherey-Nagel, Easton, PA) with 1 mL/min of 75% ammonium formate (10 mM, pH 3) and 25% acetonitrile as mobile

phase. The retention times for the (*R*) and (*S*) p-HPPH isomers were 15 and 17 min, respectively. Peak areas were directly measured and an *S/R* p-HPPH ratio was determined. Detection was by atmospheric pressure chemical ionization-mass spectrometry (APCI-MS) in the negative ion mode at an *m/z* of 266 on a Shimadzu 2010 LC-MS instrument. The APCI probe was maintained at 400 °C, the heater block at 200 °C and the desolvation line at 200 °C. The detector voltage was 1.6 kV, the microscan set to 0.3 amu, a scan time of 0.5 sec, and nitrogen gas flow rate 2.5 L/min.

***CYP2C9* Reporter plasmids.** Cloning of the -5470/+25 *CYP2C9* promoter luciferase reporter plasmid in the pGL3-basic vector (Promega, Madison, WI) has been previously described (Al-Dosari et al., 2006). The plasmid, generously supplied by Dr. Dexi Liu, Univ. Pittsburgh, was resequenced to genotype for the *CYP2C9* -3089G>A and -2663delTG and found to be WT at these two positions. Site-directed mutagenesis (SDM) was employed to create the VAR *CYP2C9* -3089A plasmid using primers in Supplemental Table 1. The *CYP2C9* -2663delTG was generated commercially by GenScript Corp. The *CYP2C9**1B haplotype was made by a performing SDM on the *CYP2C9*-2663delTG plasmid. All nucleotide variations were confirmed by DNA sequencing.

Cell culture and transient transfection assays. HepG2 human hepatoma cells were cultured in minimal essential media (MEM alpha) supplemented with 10% fetal bovine serum, 1% penicillin, and 1% streptomycin, and maintained in a humidified incubator at 37 °C in an atmosphere of 5% CO₂. For transfection studies, 3 x 10⁵ cells per well were seeded into 24 well culture dishes. After 24 h cells were transfected with 400 ng *CYP2C9* promoter luciferase reporter plasmid + 40 ng of HNF-1α and HNF-4α luciferase expression plasmids +/- 40 ng each of either pcDNA3-hPXR, pcDNA3-hCAR, pCMV6 Entry-YY1, or pCMV6

Entry-Nrf2 + pcDNA3-MafK. Each tube contained the appropriate amounts of pcDNA3 stuffer DNA to ensure equivalent amounts of total transfected plasmid and 50 ng pSV40 - LacZ to normalize LUC activity. HNF-1 α and HNF-4 α were always cotransfected because earlier observations demonstrated that these are required for optimal CYP2C9 promoter activity (Kramer et al., 2008). 24 h later, transfection medium was replaced with normal growth medium, and cells were incubated for an additional 24 h. For induction experiments, transfection medium was replaced with medium supplemented with 50 μ M PHT or DMSO. After 24 h cell lysates were prepared and luciferase assays were performed according to the manufacturer's instructions. Luciferase activities were normalized with respect to β -galactosidase activity to correct for transfection efficiency and expressed as fold change with respect to vector control. Data are reported as mean \pm S.D. of three determinations and were representative of multiple experiments. Statistical differences between groups was determined using the Student's t-test.

Electrophoretic Mobility Shift Assay (EMSA). hPXR, hCAR, hRXR, hYY1, hNrf2 and Maf K proteins were generated by TNT in vitro transcription and translation per manufacturers instructions. Proteins were incubated at 4°C for 1.5 h with ³²P-labeled double stranded oligonucleotides (6,00,000 cpm/reaction) in the presence or absence of 100-500 – fold excess of unlabeled double-stranded oligonucleotide in a DNA binding buffer (10 mM Tris pH 8.0, 40 mM KCl, 0.05% NP40, 6% glycerol, 0.2 μ g poly dI/dC, 200 μ M ZnCl₂, 1 mM dithiothreitol). Complexes were resolved by electrophoresis on a nondenaturing 6% polyacrylamide gel and analyzed using a PhosphorImager Model 860 Storm (Molecular Dynamics, Sunnyvale, CA). Specific oligonucleotides sequences used are listed in Supplemental Table 1.

PHT treatment of primary human hepatocytes. Studies in primary hepatocytes isolated from human liver were approved by the University of Pittsburgh Institutional Review Board. Livers were procured from donor organs and were flushed, in situ, and maintained with Belzar's UW solution (Barr Laboratories, Pomona, NY). Hepatocytes were isolated as previously described and were plated on collagen-coated six-well plates maintained in modified Williams' E medium for 48 h and then treated with PHT for 48 h. Media were then aspirated and TRIzol solution (Invitrogen) was added for RNA isolation. DNA was extracted from an aliquot of donor liver for CYP2C9 genotyping.

5'- rapid amplification of cDNA ends (RACE). 5'-RACE was carried out in control and PHT treated human hepatocytes extracts according to the manufacturer's protocol. The 5'RACE and CYP2C9 gene specific primers are listed in Supplemental Table 1. RACE products were analyzed using 1% agarose gel electrophoresis, cloned into a TOPO TA vector and sequenced using direct DNA sequencing.

Statistical analysis. Relationship of different genotypes with CYP2C9 mRNA expression, pHPFH (S/R) ratio, and warfarin dose requirements was analyzed using the statistical program R: A Language and Environment for Statistical Analysis (<http://www.Rproject.org>). Group differences were analyzed nonparametrically using the Wilcoxon rank sum test to compare two genotype groups whereas the Kruskal-Wallis test was used to compare three groups of genotypes with the phenotypes. Box plots indicate 2nd and 3rd quartiles, with the bold line within the box representing the median value; the whiskers represent the range after excluding the outliers. The outliers are defined by the R package as data points that fall outside the 2nd and 3rd quartiles by more than 1.5 times the interquartile range, and circles falling outside the whiskers represent outliers. Genetic association testing in the chronic

epilepsy population was performed using multiple linear regression in StataIC10 (StataCorp LP, College Station, TX, USA).

Results

To test whether a previously unrecognized SNP in *CYP2C9* might explain the paradoxically low *CYP2C9* phenytoin metabolite ratios in *CYP2C19**2 carriers, the *CYP2C9* cDNA was PCR amplified and resequenced from 12 human livers with different *CYP2C19**2 genotypes (*CYP2C19**1/*1, n=8; *CYP2C19**1/*2, n=3; and *CYP2C19**2/*2, n=1). Results demonstrated neither unique coding changes in the *CYP2C9* cDNA nor alternative *CYP2C9* transcripts that might be related to polymorphisms (e.g., intronic SNPs) (not shown).

***CYP2C9* polymorphisms in LD with *CYP2C19**2.** To identify *CYP2C9* polymorphisms in LD with *CYP2C19**2 we screened available databases and literature and identified at least eight linked *CYP2C9* polymorphisms: two intronic (intron 4 (470 bp downstream of Ex4/Int4 junction) and intron 8 (147 bp downstream of Ex8/Int8 junction)), and six in the 5' region (-76kb, -59kb, -32kb, -16kb and -3089G>A and -2663delTG). The complete haplotype has previously been designated *CYP2C9**1B (Veenstra et al., 2005). The -3089G>A and -2663delTG polymorphisms were chosen for further study because they are in proximity to binding sites at -2898, -1839 and -1818 for other *CYP2C9* transcriptional regulators (e.g., CAR, constitutive androstane receptor and PXR, pregnane X receptor) that can be activated by PHT (Fig 1B).

***CYP2C9* promoter polymorphisms are associated with maintenance PHT dose and steady-state serum levels in patients with epilepsy.** Having discovered the *CYP2C9**1B haplotype through its association with *CYP2C19**2 and its paradoxical effect on urinary p-HPPH (S)/(R) ratio, we then tested independently whether these promoter polymorphisms influenced PHT dose requirements and steady-state PHT serum levels in patients with epilepsy receiving chronic PHT therapy (n=173). After correcting for the effects of

*CYP2C9*2* and *CYP2C9*3*, gender and population structure, we found that the *CYP2C9*1B* haplotype was associated with a significant reduction in PHT dose requirements (Table 1). The effect of *CYP2C9*1B* on phenytoin dose was independent of *CYP2C9*2* and *CYP2C9*3* genotype in the linear model (Table 1). The magnitude of the effect of *CYP2C9*1B* was similar to that for the previously identified *CYP2C9*2* and *CYP2C9*3* alleles, with a beta coefficient of -42 (i.e. 42 mg lower dose requirement per minor allele carried) and significantly improved the overall predictive power of *CYP2C9* genetic markers, from (adjusted) $r^2 = 0.186$ in a model containing only *CYP2C9*2* and *CYP2C9*3* to (adjusted) $r^2 = 0.23$ in a model containing these markers plus *CYP2C9*1B*, giving an absolute difference of 4.4% of the variation in phenytoin maintenance dose explained by *CYP2C9*1B*. The independent effect of *CYP2C9*1B* is shown graphically in Figure 2 in $n = 123$ patients who do not carry a *CYP2C9*2* or *CYP2C9*3* allele.

Because body weight is also a strong independent predictor of PHT dose requirements, we re-assessed the *CYP2C9*1B* effect on PHT maintenance dose in a subset of $n=70$ patients for whom total body weight at the time of PHT therapy was recorded. After correcting for total body weight, addition of *CYP2C9*1B* to the linear model improved the fit from (adjusted) $r^2 = 0.371$ to (adjusted) $r^2 = 0.471$, with roughly 10% of the variability in PHT dose explained by this haplotype alone (Table 1). We further inspected an overlapping subset of $n=78$ patients to determine whether the effect of *CYP2C9*1B* was reflected in higher PHT serum levels in these patients. As expected, there was no relationship between the raw serum level and *CYP2C9*1B* haplotype, since the potential influence on serum level had already been corrected by the reduced maintenance dose (data not shown). However, we observed a significant effect on the ratio of serum level to maintenance dose; addition of *CYP2C9*1B* to a model including *CYP2C9*2*, **3*, gender and population structure led to

improved model fit ($p = 0.072$ without *CYP2C9*1B* vs. $p = 0.033$ in the model including *CYP2C9*1B*) (Table 2).

Neither the CYP2C9 promoter polymorphisms nor the CYP2C19*2 allele were associated with warfarin dosing requirement *in vivo*, nor hepatic CYP2C9 expression or activity *in vitro*. We next determined the generalizability of the effect of the *CYP2C19*2* genotype (and associated CYP2C9 promoter polymorphisms) on CYP2C9 mediated drug clearance of another CYP2C9 substrate, warfarin. Because a higher percentage of Asians carry the *CYP2C19*2* allele (18-23%) compared to Whites (2-5%), we turned to a Chinese population ($n=67$) with data on warfarin dose requirements necessary to achieve anticoagulation. The patients had not previously been genotyped for *CYP2C19*2* or these CYP2C9 promoter rPMs (Zhao et al., 2004). In the Hong Kong Chinese cohort, the -3089G>A and -2663delTG polymorphisms were in complete LD. However, unlike Whites, although 89% of the Chinese *CYP2C19*2* subjects also had the CYP2C9 regulatory polymorphisms, 10.7% of the Chinese *CYP2C19*2* subjects did not. Therefore, we tested for the individual effects of each of the aforementioned genotypes on warfarin dosing after excluding those patients carrying the *CYP2C9*2*, **3* and *VKORC1* variant alleles (leaving $n=46$ patients). Warfarin dosing was not correlated with either the *CYP2C19*2* genotype (not shown) or the CYP2C9 promoter polymorphisms (Fig 3A).

A human liver resource was used to determine the effect of the CYP2C9 promoter genotypes on CYP2C9 mRNA expression and phenytoin hydroxylation activity *in vitro*. Genotyping of 28 human livers from White donors confirmed that the *CYP2C9* -3089G>A and -2663delTG were in complete LD to *CYP2C19*2* in the White population (Fig 3B). Quantitative real-time PCR of CYP2C9 mRNA levels showed no significant effect of the

promoter polymorphisms on CYP2C9 basal mRNA expression. Next the (S)/(R)-p-HPPH ratios were determined in microsomes from these same livers. There was an insignificant difference in hepatic CYP2C9 activity between livers with different *CYP2C9**2 genotypes (Fig 3C) although we observed an interesting trend in this *in vitro* phenotype that was *opposite* to what was seen *in vivo*. *CYP2C9**2 heterozygote samples demonstrated a trend towards an increased S/R p-HPPH ratio which is actually what was originally expected *in vivo* (Argikar et al., 2006) because CYP2C9 is expected to contribute to PHT metabolism to a greater extent in *CYP2C9**2 poor metabolizers (Fig 1A).

To explain the *in vivo/in vitro* discrepancy we further hypothesized that the CYP2C9 promoter rPMs differentially affected PHT induction of CYP2C9 transcription. PHT is a known activator of PXR and CAR and the subjects with the paradoxical phenotype were on maintenance PHT (induction) therapy. This suggested that the measurement of urinary phenytoin metabolites *in vivo* reflected induced CYP2C9 activity and the possibility of reduced PHT autoinduction when the two CYP2C9 regulatory variant alleles were present. The -2663delTG and -3089G>A are in the vicinity of known CAR/PXR binding sites (-2898, -1839 and -1818). *In silico* bioinformatic analysis using Transfac suggested that the -3089G>A leads to the gain of a Ying Yang 1 (YY1) site and the -2663delTG leads to the loss of an Nrf2 site and Nubiscan suggested possible PXR/CAR binding sites in those same regions (Fig 1B).

Effect of individual promoter polymorphisms on constitutive and phenytoin-induced CYP2C9 promoter activity. Neither the -2663delTG nor the -3089G>A SNPs, when singly engineered into a -5470/+25-CYP2C9 luciferase reporter plasmid, decreased basal reporter activity (Fig 4A,B). Compared with the WT reference reporter, both the individual variants

decreased CAR and CAR + PHT induced CYP2C9 promoter activity (Fig 4A,B). Since the -3089G>A created a putative YY1 site, we compared the -3089G and -3089A reporter plasmids in cells in which YY1 was overexpressed with an expression plasmid. YY1 overexpression decreased the -3089A variant promoter construct to a significantly greater extent than the WT promoter construct ($p=0.04$) (Fig 4A). Since the -2663delTG destroyed a putative Nrf2 site, we compared the two reporter plasmids in cells where Nrf2 (always co-transfected with the heterodimerization partner MafK) was overexpressed. Nrf2 cotransfection significantly increased ($p=0.02$) the WT promoter construct's luciferase activity compared to the -2663delTG reporter construct, although the variant reporter was induced by PHT/Nrf2 (Fig 4B).

Effect of promoter haplotypes on constitutive and phenytoin-induced CYP2C9 promoter activity. Luciferase activity in cells with the wild-type (WT-HAP) was induced to a significantly greater extent (80% increase) compared to the variant haplotype (VAR-HAP) in cells that were co-transfected with PXR and treated with 50 μ M PHT (Fig 5A) ($p=0.002$). In contrast, co-transfection with CAR with and without PHT induced luciferase activity from the WT-HAP and VAR-HAP to similar extents (not shown). Conversely the VAR-HAP luciferase activity was 20% more repressed by YY1 overexpression alone vs. the WT-HAP cells (Fig 5B) and YY1 overexpression demonstrated a significantly greater ($p=0.007$) repression of luciferase activity in the VAR-HAP cells when cotransfected with PXR and treated with PHT.

PHT treatment of Nrf2 cotransfected cells increased luciferase promoter activity of the WT-HAP 43% more than the VAR-HAP ($p=0.02$) (Fig 5B). Nrf2 and PXR cotransfection further increased the basal ($p=0.04$) and PHT induced ($p=0.008$) promoter activity of the WT-HAP 37% more than the VAR-HAP.

Next we compared the effect of co-transfection of PXR in combination with YY1 and Nrf2. YY1 repressed activation of the WT and VAR haplotypes by either PXR or Nrf2 co-transfected plasmids, with or without PHT, although the VAR-HAP was repressed to a greater extent (up to 33%) compared to the WT-HAP (Fig 5C). In total, compared to the WT-HAP, the luciferase activity in cells containing the VAR-HAP was more significantly repressed by YY1 and less induced by PHT.

Electrophoretic mobility shift assay shows the -3089 variant allele creates a YY1 binding element. EMSAs were performed to evaluate any differential binding of YY1, Nrf2, PXR or CAR to the WT and VAR alleles. The -3089G>A was predicted to create a YY1 binding site. Only the -3089A (VAR) oligonucleotide bound YY1 (lane 12 (VAR) vs. lane 4 (WT)) and this binding was displaced by excess cold VAR oligonucleotide (Fig 6). Neither the -3089G nor the -3089A allele bound CAR:RXR or PXR:RXR heterodimers. YY1 binding appeared to be somewhat diminished by co-incubation with either heterodimer. Thus, the EMSA analysis (Fig 6A) confirmed the *in silico* prediction that the -3089A VAR allele creates a YY1 binding site. In contrast, although *in silico* bioinformatic analysis predicted that the -2663delTG destroyed an Nrf2 binding site, neither the -2663TG WT nor -2663delTG oligonucleotides bound the Nrf2:MafK heterodimer, or CAR:RXR or PXR:RXR heterodimers (not shown).

The variant CYP2C9 promoter haplotype alters CYP2C9 mRNA induction by phenytoin in primary human hepatocytes. Induction of CYP2C9 mRNA was compared in primary human hepatocytes from 12 donors (nine heterozygous for the VAR haplotype and three with a WT haplotype) treated with phenytoin. Phenytoin treatment resulted in a 3.52-fold induction of CYP2C9 mRNA in hepatocytes with the WT haplotype, but only a 2.07-

fold induction in hepatocytes with the VAR haplotype (a 42% decrease relative to the WT haplotype) (Fig 7). If the single outlier in the VAR haplotype group is removed, the difference in phenytoin induction of CYP2C9 between the two haplotypes reaches statistical significance ($p=0.02$). No difference in induction of CYP3A4 or CYP2C19 mRNAs were seen between hepatocytes with the different CYP2C9 promoter haplotypes (Fig 7).

Phenytoin treatment does not lead to induction of unique alternative *CYP2C9* mRNA transcripts.

We also considered the possibility that *CYP2C9* 5' regulatory polymorphisms could lead to genesis of PHT inducible alternative *CYP2C9* mRNAs. *CYP2C9* alternative mRNAs have been described including a chimeric transcript (*CYP2C18* exon 1-like_*CYP2C9* chimera) that contains the *CYP2C18* exon 1-like sequence spliced through a segment of the *CYP2C9* 5' UTR that is spliced to *CYP2C9* exons 2-9 (Fig 7), but does not lead to an open reading frame (Warner et al., 2001). The *CYP2C18* exon 1-like sequence is located in the intergenic region between *CYP2C9* and *CYP2C19* genes and one of the SNPs in LD to the *CYP2C19**2 allele was located at -32kb, 320 bp downstream of *CYP2C18* like exon 1. Quantitation of this spliced transcript by Q-realtime PCR in the phenytoin treated primary human hepatocytes revealed no induction of the chimera in either haplotype (Fig 7). To further exclude the possibility that some 5' regulatory SNP created a unique TF binding site (e.g., CAR or PXR) that led to use of an alternative promoter generating a unique phenytoin inducible *CYP2C9* alternative mRNA, we performed 5' RACE using cDNAs from vehicle versus phenytoin induced primary human hepatocytes. No 5' RACE product unique to the phenytoin treated hepatocytes was identified. Two transcripts of equal abundance in vehicle and PHT treated hepatocytes from both genotypes were identified by 5'-RACE. The transcripts started 25 bp (more abundant transcript) and 62 bp upstream of the translation start site. Further, when we used 5' and 3' UTR primers to amplify the full length *CYP2C9* cDNA

from control and PHT treated human hepatocytes there was no evidence by sizing of PCR products on agarose gels of any PHT inducible alternative CYP2C9 mRNAs in either genotypic group.

Discussion

We undertook this study to determine why patients with *CYP2C9*1* genotypes, but heterozygous for *CYP2C19*2*, who would be expected to produce p-HPPH(S)/(R) metabolite ratios of 30-40:1, unexpectedly produced ratios of only 12.9 (Argikar et al., 2006). We hypothesized that an unrecognized SNP in *CYP2C9*, in LD with *CYP2C19*2*, could explain this surprising finding. In Whites, we found *CYP2C19*2* was in complete LD with *CYP2C9*1B* containing the -3089G>A and -2663delTG polymorphisms. These polymorphisms decreased phenytoin-mediated induction of *CYP2C9* transcription in vitro and resulted in a diminished capacity to induce *CYP2C9* mRNA expression in primary human hepatocytes. We propose that this mechanism explains the clinically paradoxical finding of altered PHT clearance in *CYP2C19*2* Caucasian (Argikar et al., 2006) and Japanese patients (Ieiri et al., 1997) who were homozygous for *CYP2C9*1*.

In support of this, the current study demonstrates a strong effect of the *CYP2C9*1B* haplotype on PHT metabolism and dose requirements in patients with epilepsy on chronic PHT therapy. Among patients who did not carry the *CYP2C9*2* or *CYP2C9*3* alleles, the *CYP2C9*1B* haplotype was significantly associated with reduced PHT maintenance dose, consistent with reduced PHT induction of *CYP2C9* metabolism in *CYP2C9*1B* carriers. Notably, the full effect of the *CYP2C9*1B* haplotype is not appreciated unless the independent effects of *CYP2C9*2* and *CYP2C9*3* are taken into account (and vice versa). A multivariate model that includes all *CYP2C9* genotype information in addition to gender, body weight, and genomic ancestry showed that nearly half of the variation in PHT maintenance dose can be explained by these predictors (Table 1), with up to 10% of the variation in dose attributable to *CYP2C9*1B* haplotype alone. The magnitude of the effect of *CYP2C9* alleles on PHT dose requirements appeared to be strongly dependent on the clinical setting; in an additional chronic epilepsy cohort managed with a less aggressive dosing

strategy, no effect of any of the functional CYP2C9 alleles was observed (C. Depondt, personal communication).

Given the magnitude of the effect of the promoter rPMs comprising the *CYP2C9*1B* haplotype on PHT maintenance dose observed here, it may be surprising that this allele has not previously been identified in candidate gene or genome-wide association studies such as those for warfarin, another CYP2C9 substrate. However, several lines of evidence conclusively demonstrate that the promoter rPMs affecting the PHT induction phenotype do not decrease basal CYP2C9 expression: neither hepatic *CYP2C9* mRNA expression nor activity were affected by the *CYP2C19*1B* genotypes; and warfarin maintenance dose was not significantly affected by the -3089G>A and -2663delTG polymorphisms in Chinese patients (Fig 3A). Likewise, Veenstra et al. (2005) previously found no difference in warfarin sensitivity (basal CYP2C9 activity) in White patients with the *CYP2C9*1B* allele.

Although we identified the -3089G>A and -2663delTG CYP2C9 promoter rPMs by searching for SNPs in LD to *CYP2C19*2*, these rPMs were previously identified in the *CYP2C9*1B* promoter haplotype (allele frequency 17.45% Whites of European descent). Recently Kramer et al. (2008) identified common haplotypes in Hispanics and designated this same allele *CYP2C9*1D* (hereafter referred to as *Kramer *1D* when referencing results from that publication). Notably, in transient transfection studies the *Kramer *1D* haplotype, relative to the reference haplotype, exhibited no difference in constitutive promoter activity but showed a 50% decrease in PXR mediated promoter activity upon treatment with rifampin. This result is similar to the effect observed here, that the *CYP2C9*1B* promoter had diminished activation by phenytoin. The *Kramer *1D* haplotype also includes a -1188T>C SNP. Although we did not include this SNP in our CYP2C9 variant reporters, Kramer et al. (2008) deduced that the -1188T>C transition was unlikely to be singly responsible for the differences in induction profiles because it was present in numerous other haplotypes that

behaved no differently from the reference allele with respect to either basal or rifampin-inducible activity. Further, a report by Sandberg et al. (2004) found no effect of the -1188T>C variant on gene expression in vitro. Although we cannot exclude the possibility that the -1188T>C might contribute to our phenotype, it would not negate the contribution of -3089G>A or -2663delTG, it would simply imply that these polymorphisms are not the only ones contributing to decreased phenytoin-mediated CYP2C9 induction.

Phenytoin has been shown to activate both PXR and CAR (Wang et al., 2004; Yueh et al., 2005; Luo et al., 2002). Although Nubiscan predicted possible PXR or CAR binding elements around -3089 and -2663 (Fig 1), neither receptor bound to the -3089 or -2663 wild-type or variant oligonucleotides and hence cannot explain the decreased induction response. Nevertheless, the VAR-HAP demonstrated a significantly decreased PXR mediated PHT induction of promoter activity compared to the WT-HAP (Fig 5). It is also possible that CAR contributes to the differential activation of the CYP2C9 WT and VAR promoters by phenytoin because the CYP2C9 WT reporter was induced to a greater extent by co-transfected CAR compared to reporters with single CYP2C9 promoter variations (Fig 4). Although it is unclear why the single variant reporters were more induced by CAR +/- PHT while the haplotype reporters were more induced by PXR +/- PHT, it does not negate the fact that the variant allele was consistently less inducible by PHT.

There are Ying Yang (YY1) binding sites predicted in the CYP2C9 5'-flanking region and the -3089G>A polymorphism created an additional YY1 binding site. YY1 is a transcription factor that can either induce or repress expression, depending upon the target gene. We found YY1 is a repressor of PHT inducible CYP2C9 transcription, but the magnitude of repression was always greater in the CYP2C9 variant reporter with the additional YY1 site. The results suggest that YY1 contributes to the diminished PHT inducibility of the *1B genotype.

Our data support the idea that PHT activation of Nrf2 could participate in CYP2C9 induction. PHT-activated Nrf2 induces mRNA expression of protective enzymes by binding to antioxidant response elements (ARE) in the promoter of target genes. Although Transfac predicted that the -2663delTG abrogated a putative Nrf2 binding site, EMSA failed to demonstrate Nrf2:MafK binding to oligonucleotides with the -2663TG or TGdeletion sequences. Nevertheless, it is still possible that Nrf2 contributes to PHT induction of CYP2C9 because (a) mice treated with PHT showed Keap1-Nrf2-dependent induction of genes that included *Cyp2b10* and *Cyp2c29* (Lu et al., 2008; Lu and Uetrecht, 2008); (b) Transfac analysis showed 21 high scoring putative ARE binding sites in the -5.3 kb CYP2C9 5' flanking sequence; and (c) co-transfection with Nrf2/MafK induced luciferase activity from the CYP2C9 reporter plasmids. If PHT generates an antioxidant response signal it could be due to PHT metabolites activating the Keap1-Nrf2-ARE signaling pathway.

The low p-HPPH(S)/(R) ratio in *CYP2C19*2* carriers appears to be due to the lower induction of the linked *CYP2C9*1B* allele, and resulting decreased metabolism of PHT to (S)-pHPPH, even in the face of the greatly diminished formation of (R)-p-HPPH by *CYP2C19*2*. We could find no other polymorphism in the CYP2C9 cDNA of *CYP2C19*2/CYP2C9*1B* carriers, nor generation of any novel PHT induced alternative CYP2C9 transcripts in human hepatocytes with these genotypes that could explain the lower (S)-p-HPPH or greater (R) metabolite formation. Likewise, 5'RACE of PHT-treated primary human hepatocytes failed to identify any differentially activated promoter/CYP2C9 transcripts in *CYP2C19*2* subjects. Although we considered the possibility that PHT induction of other metabolic enzymes might contribute to the observed alteration in (S)/(R)-p-HPPH ratios in *CYP2C19*2* patients, the literature strongly supports that p-HPPH is formed almost exclusively by either CYP2C9 or CYP2C19, with negligible activity by expressed CYP1A2, 2A6, 2B6, 2C8, 2D6, 2E1 or 3A4 (Giancarlo et al., 2001; Komatsu et al.,

2000). p-HPPH can undergo a second hydroxylation to form a catechol metabolite (Midha et al., 1977). This can also be formed via the diol metabolite by dihydrodiol dehydrogenase. Catechol formation from p-HPPH appears to be mainly catalyzed by CYP2C19 with additional contribution from CYP3A4 and CYP2C9 (Cuttle et al., 2000). In vivo, the catechol and methylcatechol metabolites are minor accounting for <5% of the dose in the urine. Although the amounts of these other metabolites were not measured in our study, the differential formation of these metabolites, even if they occurred, would appear insufficient to account for the altered p-HPPH ratios observed in *CYP2C19**2 patients.

The finding that the *CYP2C9**1*B* allele has diminished PHT inducibility is clinically relevant because PHT has been reported to undergo auto-induction (Miller et al., 1989; Chetty et al., 1998; Dickinson et al., 1985). Miller et al. (1989) reported two patients who demonstrated an 11-20% increase in Vmax after 5 months-1 yr treatment with PHT. Others have reported modest induction of PHT clearance and a decrease in AUC after repeated doses of PHT (Chetty et al., 1998; Yuen et al., 1983). Dickinson et al. (1985) found that eight healthy individuals demonstrated a significant auto-induction of PHT metabolism and urinary excretion of p-HPPH increased with repeated administration of PHT. While PHT auto-induction is not as generally appreciated clinically as is the case for another antiepileptic drug, carbamazepine, this may potentially be explained by reduced CYP2C9 inducibility in patients carrying the *CYP2C9**1*B* haplotype, which may obscure the PHT auto-induction in studies that have not accounted for this genetic effect.

Our findings, combined with those of Kramer et al. (2008), suggest that the *CYP2C9**1*B* allele will not only affect the magnitude of PHT autoinduction of clearance but also the magnitude of other CYP2C9 drug-drug interactions resulting from PXR/CAR activation. CYP2C9 metabolizes approximately 16% of clinically important drugs, including some with narrow therapeutic indices: sulfonylureas such as tolbutamide, anticonvulsants

such as phenytoin and the anticoagulant warfarin. Other substrates include the antihypertensive losartan, the NSAIDs ibuprofen, naproxen, and flurbiprofen and drugs such as fluvastatin, fluoxetine and rosiglitazone. Thus, it is possible that the extent of drug interactions following co-treatment with known PXR/CAR activators and CYP2C9 inducers such as rifampin or phenytoin or barbiturates might differ between individuals with the *CYP2C9*1B* vs. other *CYP2C9*1* genotypes. Although CYP2C9 is not highly induced in human hepatocytes by phenytoin (Sahi et al., 2009) and (Fig 7), hepatic CYP2C9 is also induced by rifampin, phenobarbital and avasimibe (Sahi et al., 2009; Chen et al., 2004). Moreover, CYP2C9 is among the three most highly induced CYPs in human duodenum in patients treated with clinical doses of oral rifampin (E. Schuetz, unpublished observation). Our results would suggest that the magnitude of drug interactions are likely to be different between the 17.4% of Whites and 6.6% of Hispanics (Kramer et al., 2008) with the *CYP2C9*1B* allele compared to those with other *CYP2C9*1* alleles.

Acknowledgements

We thank the Hartwell center for DNA sequencing and oligonucleotide synthesis. We thank Rinki Singh for her assistance in collection of clinical data.

References

- Al-Dosari MS, Knapp JE and Liu D (2006) Activation of human CYP2C9 promoter and regulation by CAR and PXR in mouse liver. *Mol Pharm* **3**:322-328.
- Argikar UA, Cloyd JC, Birnbaum AK, Leppik IE, Conway J, Kshirsagar S, Oetting WS, Klein EC and Remmel RP (2006) Paradoxical urinary phenytoin metabolite (S)/(R) ratios in CYP2C19*1/*2 patients. *Epilepsy Res* **71**:54-63.
- Aynacioglu AS, Brockmoller J, Bauer S, Sachse C, Guzelbey P, Ongen Z, Nacak M and Roots I (1999) Frequency of cytochrome P450 CYP2C9 variants in a Turkish population and functional relevance for phenytoin. *Br J Clin Pharmacol* **48**:409-415.
- Bajpai M, Roskos LK, Shen DD and Levy RH (1996) Roles of cytochrome P4502C9 and cytochrome P4502C19 in the stereoselective metabolism of phenytoin to its major metabolite. *Drug Metab Dispos* **24**:1401-1403.
- Bhasker CR, Miners JO, Coulter S and Birkett DJ (1997) Allelic and functional variability of cytochrome P4502C9. *Pharmacogenetics* **7**:51-58.
- Browne TR and Leduc B (2002). Phenytoin and other hydantoins: chemistry and biotransformation. In *Anti-epileptic Drugs* 5th edn. (Levy RH, Mattson RH, Meldrum BS and Perucca E eds) pp 565–580, Lippincott Williams and Wilkins, Philadelphia.
- Chen Y, Ferguson SS, Negishi M and Goldstein JA (2004) Induction of human CYP2C9 by rifampicin, hyperforin, and phenobarbital is mediated by the pregnane X receptor. *J Pharmacol Exp Ther* **308**:495-501.
- Chetty M, Miller R and Seymour MA (1998) Phenytoin auto-induction. *Ther Drug Monit* **20**:60-62.

- Cuttle L, Munns AJ, Hogg NA, Scott JR, Hooper WD, Dickinson RG and Gillam EM (2000) Phenytoin metabolism by human cytochrome P450: involvement of P450 3A and 2C forms in secondary metabolism and drug-protein adduct formation. *Drug Metab Dispos* **28**:945-950.
- de Moraes SM, Wilkinson GR, Blaisdell J, Nakamura K, Meyer UA and Goldstein JA (1994) The major genetic defect responsible for the polymorphism of S-mephenytoin metabolism in humans. *J Biol Chem* **269**:15419-15422.
- Desta Z, Zhao X, Shin JG and Flockhart DA (2002) Clinical significance of the cytochrome P450 2C19 genetic polymorphism. *Clin Pharmacokinet* **41**:913-958.
- Dickinson RG, Hooper WD, Patterson M, Eadie MJ and Maguire B (1985) Extent of urinary excretion of p-hydroxyphenytoin in healthy subjects given phenytoin. *Ther Drug Monit* **7**:283-289.
- Garrard J, Harms SL, Eberly LE and Leppik IE (2007) Use of antiepileptic medications in nursing homes. *Int Rev Neurobiol* **81**:165-182.
- Giancarlo GM, Venkatakrishnan K, Granda BW, von Moltke LL and Greenblatt DJ (2001) Relative contributions of CYP2C9 and 2C19 to phenytoin 4-hydroxylation in vitro: inhibition by sulfaphenazole, omeprazole, and ticlopidine. *Eur J Clin Pharmacol* **57**:31-36.
- Ieiri I, Mamiya K, Urae A, Wada Y, Kimura M, Irie S, Amamoto T, Kubota T, Yoshioka S, Nakamura K, Nakano S, Tashiro N and Higuchi S (1997) Stereoselective 4'-hydroxylation of phenytoin: relationship to (S)-mephenytoin polymorphism in Japanese. *Br J Clin Pharmacol* **43**:441-445.

- Komatsu T, Yamazaki H, Asahi S, Gillam EM, Guengerich FP, Nakajima M and Yokoi T (2000) Formation of a dihydroxy metabolite of phenytoin in human liver microsomes/cytosol: roles of cytochromes P450 2C9, 2C19, and 3A4. *Drug Metab Dispos* **28**:1361-1368.
- Kramer MA, Rettie AE, Rieder MJ, Cabacungan ET and Hines RN (2008) Novel CYP2C9 promoter variants and assessment of their impact on gene expression. *Mol Pharmacol* **73**:1751-1760.
- Kupfer A and Preisig R (1984) Pharmacogenetics of mephenytoin: a new drug hydroxylation polymorphism in man. *Eur J Clin Pharmacol* **26**:753-759.
- Leppik IE (2007) Epilepsy in the elderly: scope of the problem. *Int Rev Neurobiol* **81**:1-14.
- Lu W, Li X and Uetrecht JP (2008) Changes in gene expression induced by carbamazepine and phenytoin: testing the danger hypothesis. *J Immunotoxicol* **5**:107-113.
- Lu W and Uetrecht JP (2008) Peroxidase-mediated bioactivation of hydroxylated metabolites of carbamazepine and phenytoin. *Drug Metab Dispos* **36**:1624-1636.
- Luo G, Cunningham M, Kim S, Burn T, Lin J, Sinz M, Hamilton G, Rizzo C, Jolley S, Gilbert D, Downey A, Mudra D, Graham R, Carroll K, Xie J, Madan A, Parkinson A, Christ D, Selling B, LeCluyse E and Gan LS (2002) CYP3A4 induction by drugs: correlation between a pregnane X receptor reporter gene assay and CYP3A4 expression in human hepatocytes. *Drug Metab Dispos* **30**:795-804.
- Miller R, Bill PL and Du TJ (1989) Phenytoin auto-induction? Case reports. *S Afr Med J* **75**:332-333.

- Rettie AE, Haining RL, Bajpai M and Levy RH (1999) A common genetic basis for idiosyncratic toxicity of warfarin and phenytoin. *Epilepsy Res* **35**:253-255.
- Sahi J, Shord SS, Lindley C, Ferguson S and LeCluyse EL (2009) Regulation of cytochrome P450 2C9 expression in primary cultures of human hepatocytes. *J Biochem Mol Toxicol* **23**:43-58.
- Sandberg M, Johansson I, Christensen M, Rane A and Eliasson E (2004) The impact of CYP2C9 genetics and oral contraceptives on cytochrome P450 2C9 phenotype. *Drug Metab Dispos* **32**:484-489.
- Stubbins MJ, Harries LW, Smith G, Tarbit MH and Wolf CR (1996) Genetic analysis of the human cytochrome P450 CYP2C9 locus. *Pharmacogenetics* **6**:429-439.
- Sullivan-Klose TH, Ghanayem BI, Bell DA, Zhang ZY, Kaminsky LS, Shenfield GM, Miners JO, Birkett DJ and Goldstein JA (1996) The role of the CYP2C9-Leu359 allelic variant in the tolbutamide polymorphism. *Pharmacogenetics* **6**:341-349.
- Tate SK, Depondt C, Sisodiya SM, Cavalleri GL, Schorge S, Soranzo N, Thom M, Sen A, Shorvon SD, Sander JW, Wood NW and Goldstein DB (2005) Genetic predictors of the maximum doses patients receive during clinical use of the anti-epileptic drugs carbamazepine and phenytoin. *Proc Natl Acad Sci U S A* **102**:5507-5512.
- Veenstra DL, Blough DK, Higashi MK, Farin FM, Srinouanprachan S, Rieder MJ and Rettie AE (2005) CYP2C9 haplotype structure in European American warfarin patients and association with clinical outcomes. *Clin Pharmacol Ther* **77**:353-364.

- Wang H, Faucette S, Moore R, Sueyoshi T, Negishi M and LeCluyse E (2004) Human constitutive androstane receptor mediates induction of CYP2B6 gene expression by phenytoin. *J Biol Chem* **279**:29295-29301.
- Warner SC, Finta C and Zaphiropoulos PG (2001) Intergenic transcripts containing a novel human cytochrome P450 2C exon 1 spliced to sequences from the CYP2C9 gene. *Mol Biol Evol* **18**:1841-1848.
- Yueh MF, Kawahara M and Raucy J (2005) High volume bioassays to assess CYP3A4-mediated drug interactions: induction and inhibition in a single cell line. *Drug Metab Dispos* **33**:38-48.
- Yuen GJ, Bell RD and Ludden TM (1983) Phenytoin cumulation profiles. *Res Commun Chem Pathol Pharmacol* **42**:355-368.
- Zhao F, Loke C, Rankin SC, Guo JY, Lee HS, Wu TS, Tan T, Liu TC, Lu WL, Lim YT, Zhang Q, Goh BC and Lee SC (2004) Novel CYP2C9 genetic variants in Asian subjects and their influence on maintenance warfarin dose. *Clin Pharmacol Ther* **76**:210-219.

Footnotes

a) *Authorship note: Amarjit S. Chaudhry and Thomas J. Urban contributed equally to this work.

b) This work was supported by the National Institutes of Health National Institute of General Medical Sciences [Grants GM60346, GM61393]; the National Institutes of Health National Cancer Institute [Cancer Center Support Grant P30 CA21765]; the National Institutes of Health Neurological Disorders and Stroke [Grant P50 NS16308]; the National Institutes of Health National Institute of Diabetes and Digestive and Kidney Diseases [Contract #N01-DK-9-2310]; the Wellcome Trust [Grant 084730]; the UK Medical Research Council [Grant G0400126]; a Postdoctoral Research Fellowship from the American Epilepsy Society; the National Society for Epilepsy; the American Lebanese Syrian Associated Charities (ALSAC); the Research Grants Council of the Hong Kong Special Administrative Region, China [Project no. CUHK4519/06M]; the UCLH CDRC grant (F136); and this work was partly undertaken at UCLH/UCL who received a proportion of funding from the UK Department of Health's NIHR Biomedical Research Centre's funding scheme.

c) Person to receive reprint requests: Erin Schuetz, Ph.D. Department of Pharmaceutical Sciences, 262 Danny Thomas Place, St. Jude Children's Research Hospital, Memphis, TN-38105; Phone: (901) 595-2205; FAX: (901) 595-3125
Email: erin.schuetz@stjude.org

Legends for Figures

Figure 1. A) PHT is metabolized to a mixture of (*S*) and (*R*)-pHPPH by CYP2C9 and CYP2C19. CYP2C9 has a major contribution to this enantioselective metabolism and preferentially forms (*S*)-pHPPH with a urinary (*S*)/(*R*)-pHPPH ratio of 40:1 compared to CYP2C19 that forms both enantiomers equally and gives a ratio of 1:1. B) Putative TF and nuclear receptor binding sites in or near the -2663delTG and -3089G>A are shown. YY1 and Nrf2 binding sites are underlined and bolded. A CYP2C9 promoter map indicates the location of these polymorphisms and known CAR/PXR binding sites (-2898, -1839 and -1818) (solid triangles).

Figure 2. *CYP2C9*1B* haplotype is associated with PHT maintenance dose in patients with epilepsy. The box plot shows only those patients found to be non-carriers of the reduced-function *CYP2C9*2* and *CYP2C9*3* alleles. A linear trend of decreased PHT dose requirements with increasing number of *CYP2C9*1B* alleles was observed. **p* = 0.017 vs. *CYP2C9*1/*1*; ***p* = 0.060 vs. *CYP2C9*1/*1B*.

Figure 3. A) Effect of -3089G>A on warfarin dosing in a cohort of 46 Chinese patients on warfarin therapy after excluding samples with *CYP2C9*2* and *3 and *VKORC1* variant alleles. B) *CYP2C9* mRNA expression in 28 human livers analyzed by Q-real-time PCR. Y-axis depicts mRNA expression each liver (normalized to its GAPDH and this value depicted relative to the normalized value obtained for one liver arbitrarily set at 100%). The x-axis represents visual genotyping results for each polymorphism. Light gray squares represent homozygous major, dark gray heterozygous and black homozygous minor allele. Box plot in

inset depicts the effect of -3089G>A on mRNA expression after excluding *CYP2C9**2 and *3 samples. C) Effect of -3089G>A on the *in vitro* formation of (S) and (R)-pHPPH in fourteen human liver microsome samples after excluding samples with *CYP2C9**2 and *3. Group differences were analyzed nonparametrically using the Wilcoxon rank sum test to compare two genotypes with the phenotype. Box plots indicate 2nd and 3rd quartiles. The bold line within the box represents median and whiskers represent the range after excluding the outliers.

Figure 4. Effect of individual *CYP2C9* promoter polymorphisms on basal and PHT inducible promoter activity. HepG2 cells were transfected with *CYP2C9* reporters (A) -3089A and -3089G, and (B) -2663TG and -2663delTG with or without co-transfected PXR, CAR, YY1 or NRF2 expression plasmids and luciferase expression measured after treatment with vehicle or PHT for 24 hrs. Luciferase activities were normalized to β -galactosidase. The relative luciferase normalized activity in vehicle treated cells were each set as one, and the fold change in relative luciferase activity with respect to vector (w.r.t.) was graphed relative to this baseline. Values represent the mean \pm S.D. measured in triplicate. P values indicate where there is a significant difference between the fold change in the variant allele compared with the corresponding wild-type allele for the identical condition, *p=0.05, **p=0.02, ***p=0.03, #p=0.007, ##p=0.0005, ###p=0.005.

Figure 5. The *CYP2C9* variant haplotype shows diminished responsiveness to PHT induction *in vitro* and *in vivo*. A-C) HepG2 cells were transfected with *CYP2C9* WT and VAR-HAP reporters +/- PXR, YY1 or Nrf2 expression plasmids, and luciferase expression measured after treatment with vehicle or PHT for 24 hrs. Results were analyzed and graphed as in Figure 4 legend. P values indicate significant differences between the fold change in the VAR-HAP

compared with the corresponding WT-HAP for the identical condition, * $p=0.04$, ** $p=0.02$,
$p=0.007$, ## $p=0.005$, ### $p=0.002$.

Figure 6. EMSA of transcription factor binding to the wild-type and polymorphic CYP2C9 YY1 promoter elements. 32 P-labeled oligonucleotides representing the -3089G and A were incubated with products from in vitro synthesis with the empty expression vector (pcDNA3), or synthesized PXR:RXR, CAR:RXR and YY1 proteins in the absence (no competitor) or presence of increasing amounts of unlabeled oligonucleotide cold competitor (CC). After electrophoresis, complex formation was assessed by a phosphorimager. Lanes 17, 18 & 19 represent binding of YY1, CAR and PXR to positive control (+ve Ctrl) oligonucleotides, respectively. Sequences for all oligonucleotides are provided in Supplemental Table 1.

Figure 7. Effect of CYP2C9 promoter genotypes on CYP expression in human hepatocytes treated with PHT. Primary human hepatocytes were treated with vehicle or PHT for 48 hrs, RNA extracted and analyzed by quantitative real-time PCR. CYP2C9 and CYP2C18 like Ex1/ 2C9 Ex2 chimeric transcripts were amplified from cDNA using specific primers as shown. The fold change of each mRNA after PHT treatment is depicted on the y axis and CYP2C9 -3089G>A genotypes on the x axis. Group differences were analyzed nonparametrically using the Wilcoxon rank sum test as described in Figure 3 legend.

Table 1. Association of CYP2C9 variants with PHT maintenance dose

Model	Independent Variables	Beta Coefficient	Adjusted R ²	F	p-value
1	<i>CYP2C9</i> *2	-44.6	0.113	3.44	0.004
2	<i>CYP2C9</i> *3	-89.0	0.143	4.20	6.71 X 10 ⁻⁵
3	<i>CYP2C9</i> *1B	-21.7	0.080	2.66	0.121
4	<i>CYP2C9</i> *2 + <i>CYP2C9</i> *3	-45.2 -89.6	0.186	4.94	3.09 X 10 ⁻⁶
5	<i>CYP2C9</i> *2 + <i>CYP2C9</i> *3 + <i>CYP2C9</i> *1B	-105.4 -52.6 -42.2	0.230	5.67	1.11 X 10 ⁻⁷
6	TBW + <i>CYP2C9</i> *2 + <i>CYP2C9</i> *3 +	2.52 -47.9 -93.2	0.371	5.06	2.70 X 10 ⁻⁵
7	TBW + <i>CYP2C9</i> *2 + <i>CYP2C9</i> *3 + <i>CYP2C9</i> *1B	2.29 -65.5 -121 -66.4	0.471	6.59	5.4 X 10 ⁻⁷

Effects of *CYP2C9* alleles on PHT dose were estimated by linear regression in a multivariate model including gender and ancestry estimated according to a principal components method (EIGENSTRAT). The test sample included n = 173 patients with epilepsy receiving maintenance PHT therapy, except for models 6 and 7 which included only a subset of n = 70 patients with known body weight at the time of PHT maintenance therapy.

Table 2. Association of CYP2C9 variants with PHT serum levels normalized to PHT maintenance dose

Model	Independent Variables*	Adjusted R ²	p-value
1	<i>CYP2C9*2</i>	0.081	0.084
2	<i>CYP2C9*3</i>	-0.063	0.899
3	<i>CYP2C9*1B</i>	-0.071	0.936
4	<i>CYP2C9*2</i> + <i>CYP2C9*3</i>	0.092	0.072
5	<i>CYP2C9*2</i> + <i>CYP2C9*3</i> + <i>CYP2C9*1B</i>	0.129	0.033

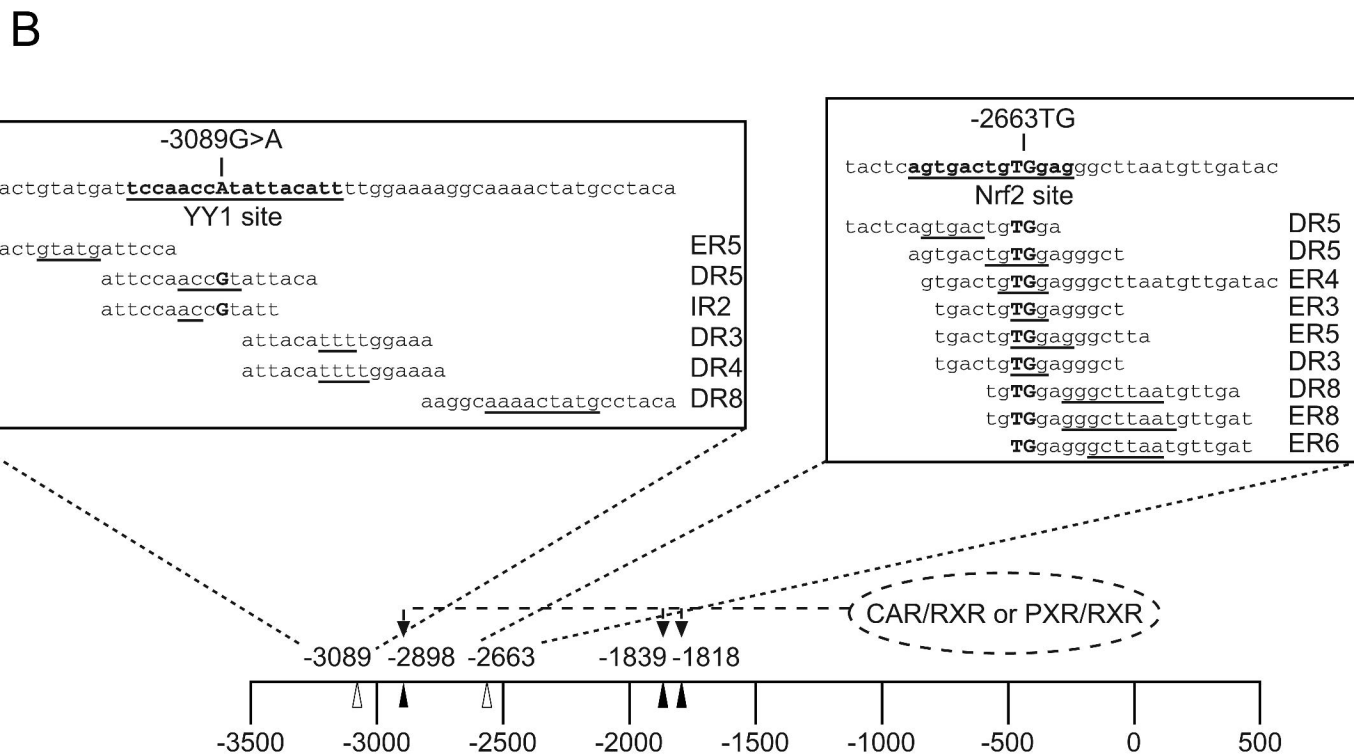
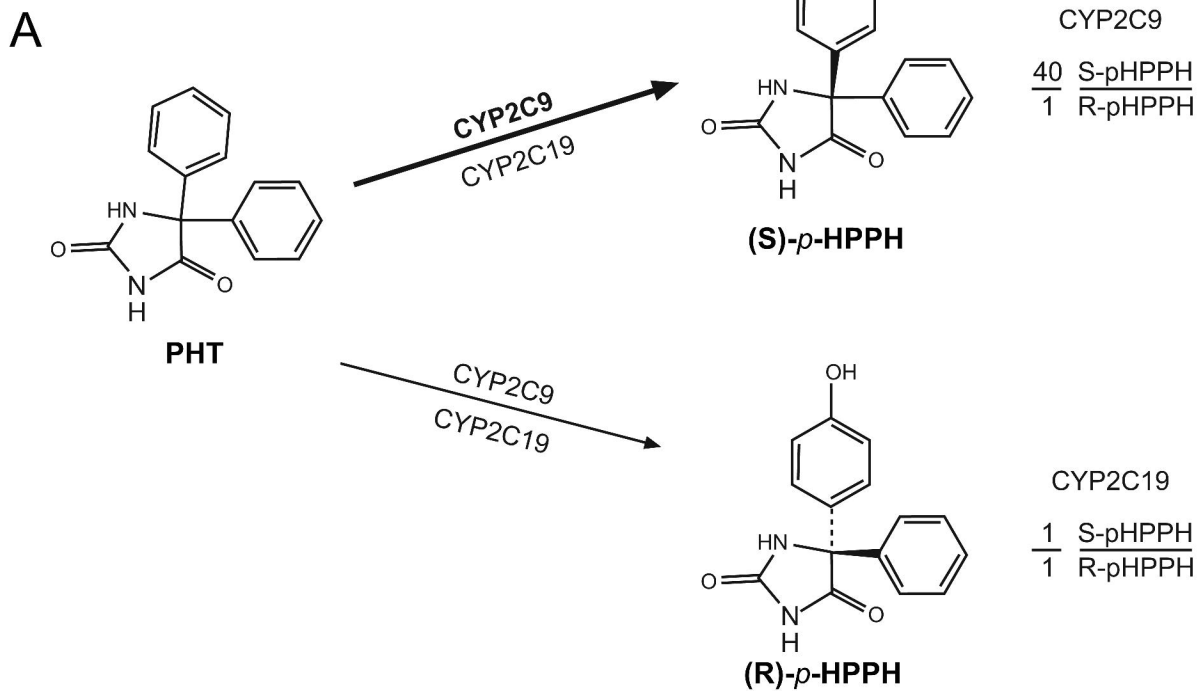


Figure 1

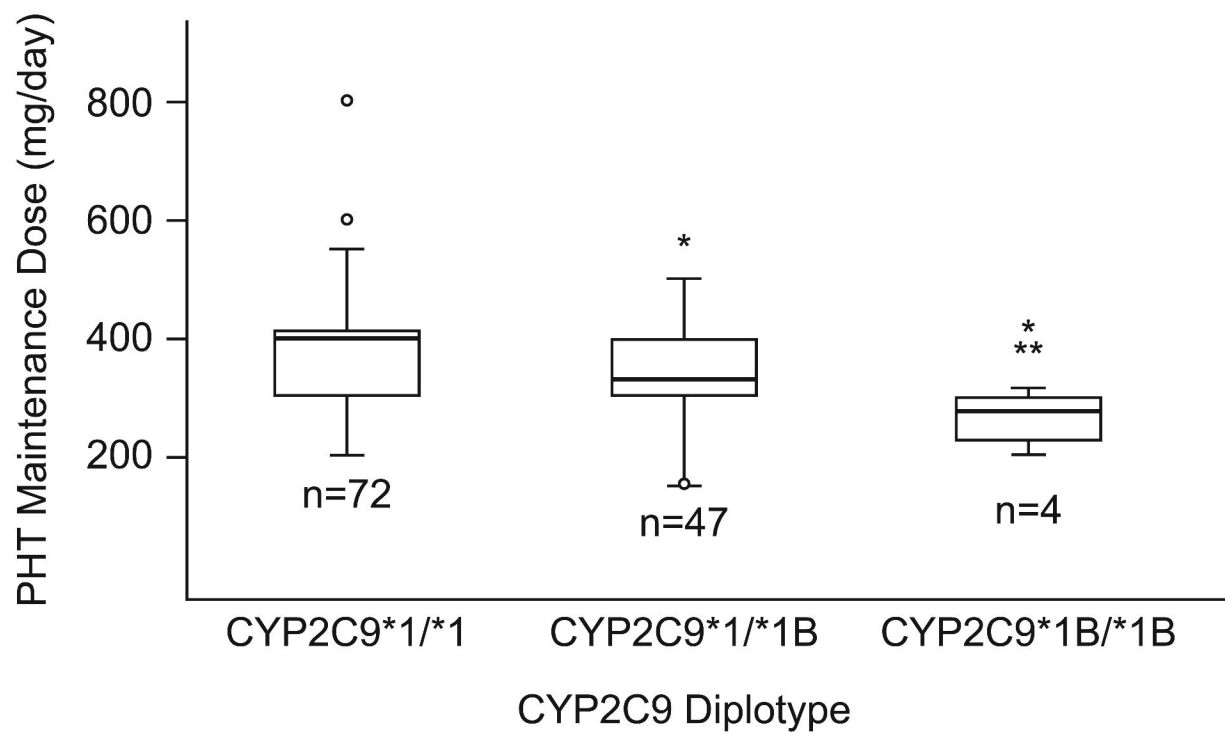


Figure 2

log warfarin dose

WT for CYP2C9*2
WT for CYP2C9*3
WT for VKORC1

CYP2C9 -3089G>A

CYP2C9 -3089G>A	n	Median log warfarin dose	Q1	Q3	Min	Max
AA	3	0.50	0.34	0.52	0.18	0.54
GA	17	0.40	0.35	0.54	0.30	0.70
GG	26	0.48	0.30	0.54	0.18	0.78

Figure 2 consists of a main bar chart and an inset box plot. The main bar chart displays CYP2C9 mRNA levels for 30 patients, sorted by increasing levels. The y-axis is labeled 'CYP2C9 mRNA' and ranges from 0% to 600%. The x-axis represents 30 individual patients. A legend at the bottom indicates the frequency of variants: Major (light gray), HET (medium gray), and Minor (black). The inset box plot shows the distribution of mRNA levels for patients with AA, GA, and GG genotypes. The y-axis for the inset ranges from 0 to 400. The x-axis for the inset is labeled with genotypes: AA, GA, and GG.

WT for CYP2C9*2
WT for CYP2C9*3

pHPH (S/R) ratio

CYP2C9 -3089G>A → GG n=7 GA n=7

Figure 3

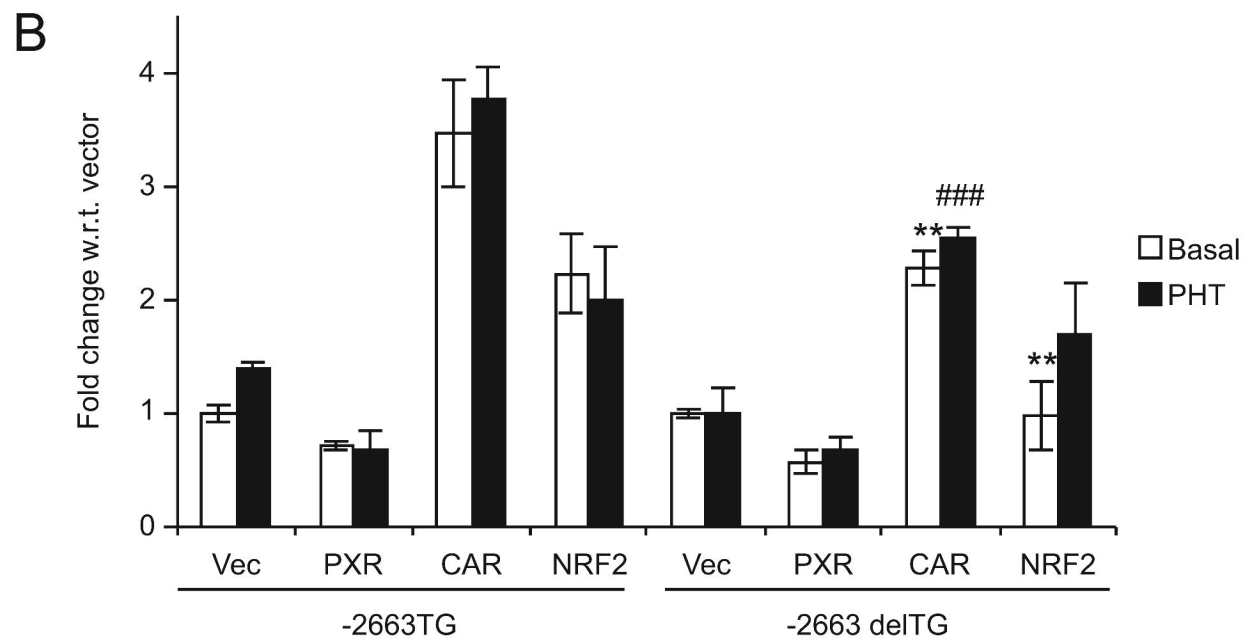
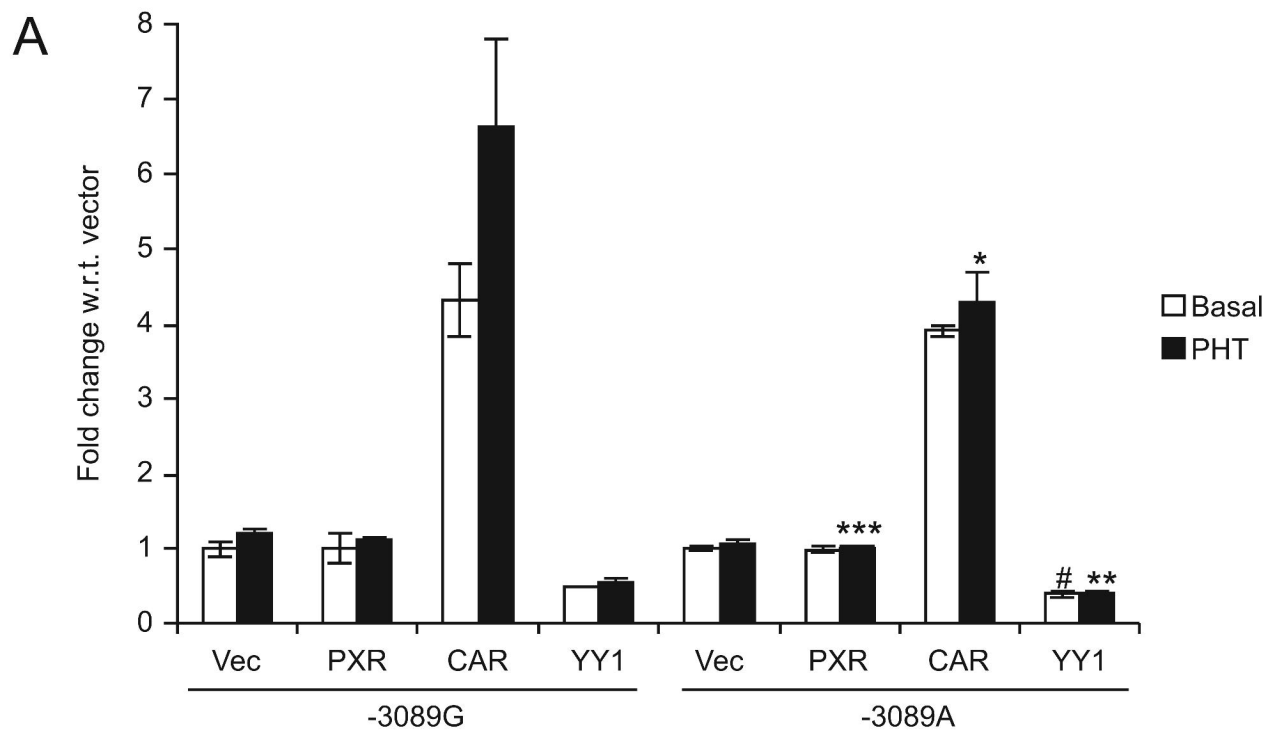


Figure 4

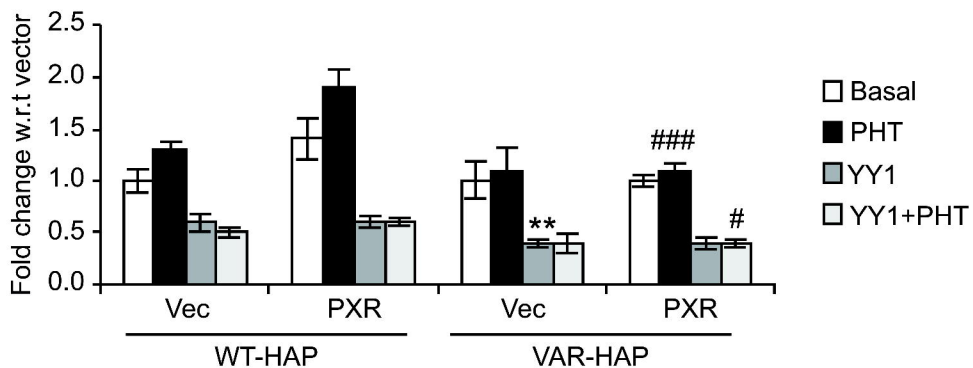
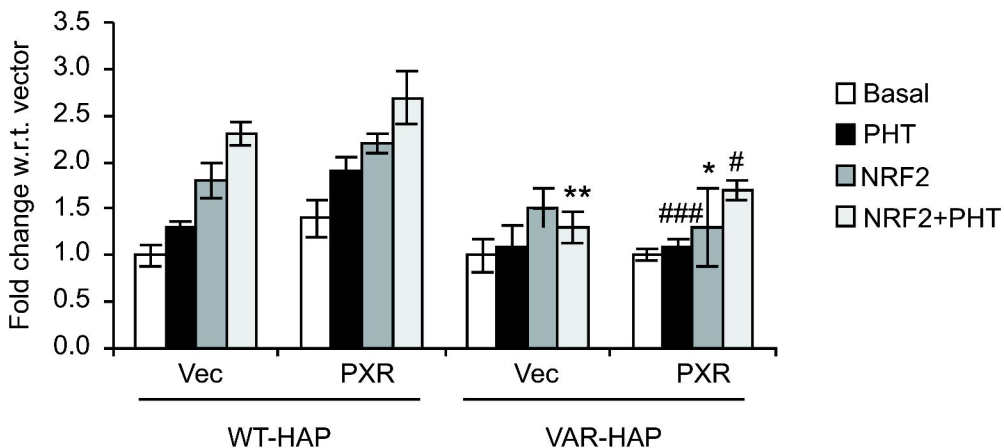
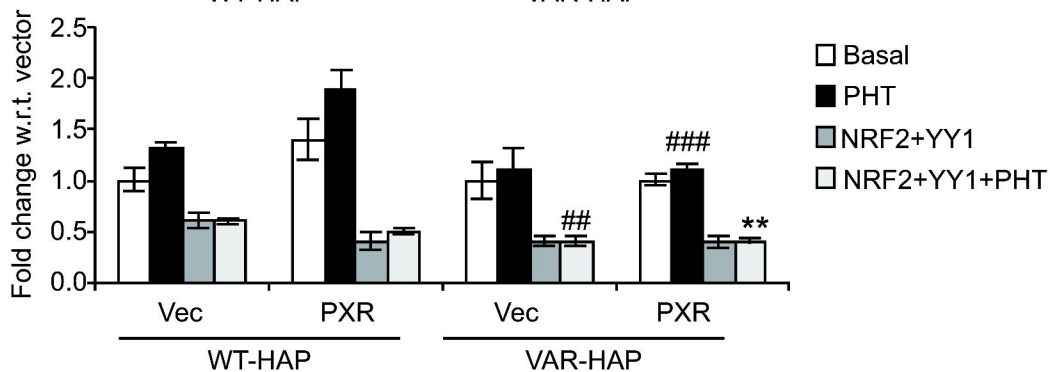
A**B****C**

Figure 5

	WT-3089G								VAR-3089A								+ve Ctrl		
pcDNA3	+	-	-	-	-	-	-	-	+	-	-	-	-	-	-	-	-	-	
PXR/RXR	-	+	-	-	-	-	+	-	-	+	-	-	-	-	+	-	-	+	
CAR/RXR	-	-	+	-	-	-	-	+	-	-	+	-	-	-	-	+	-	+	
YY1	-	-	-	+	+	+	+	+	-	-	-	+	+	+	+	+	+	-	
CC→	<div><div></div><div></div><div></div><div></div><div></div><div></div><div></div><div></div></div>								<div><div></div><div></div><div></div><div></div><div></div><div></div><div></div><div></div></div>										
	1	2	3	4	5	6	7	8	9	10	11	12	13	14	15	16	17	18	19

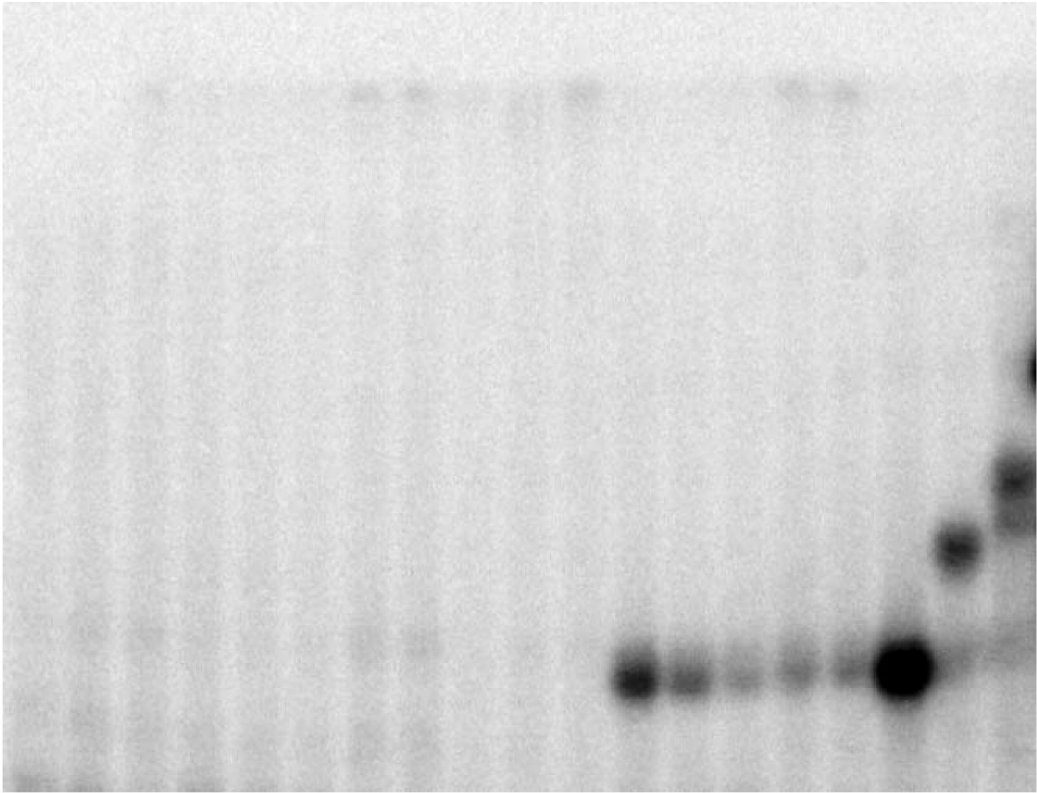


Figure 6

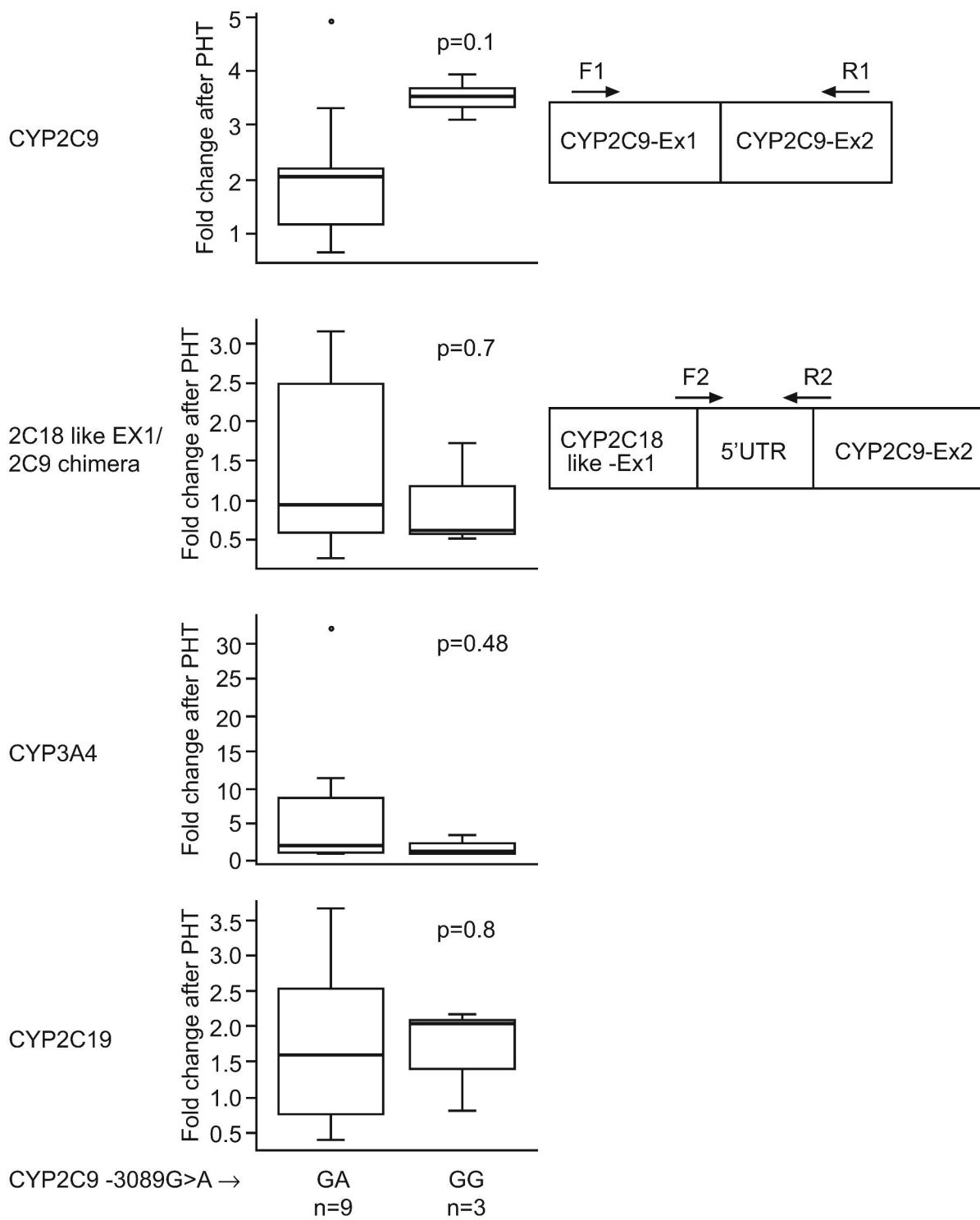


Figure 7